Available online at www.sciencedirect.com
ScienceDirect
Journal of Theoretical Biology 242 (2006) 598–606
Journal of Theoretical Biology
www.elsevier.com/locate/yjtbi

A mathematical analysis of the dynamics of prion proliferation

Meredith L. Greer[a], Laurent Pujo-Menjouet[b], Glenn F. Webb[c,*]

[a]Department of Mathematics, Bates College, 213 Hathorn Hall Bates College, Lewiston, Maine 04240, USA
[b]Institut Camille Jordan, Université Claude Bernard Lyon 1, 43 boulevard du 11 Novembre 1918, 69622 Villeurbanne cedex, France
[c]Department of Mathematics, Vanderbilt University, 1326 Stevenson Center, Nashville, TN 37240-0001, USA

Received 4 October 2005; received in revised form 3 April 2006; accepted 12 April 2006
Available online 28 April 2006

Abstract

How do the normal prion protein (PrP^C) and infectious prion protein (PrP^{Sc}) populations interact in an infected host? To answer this question, we analyse the behavior of the two populations by studying a system of differential equations. The system is constructed under the assumption that PrP^{Sc} proliferates using the mechanism of nucleated polymerization. We prove that with parameter input consistent with experimentally determined values, we obtain the persistence of PrP^{Sc}. We also prove local stability results for the disease steady state, and a global stability result for the disease free steady state. Finally, we give numerical simulations, which are confirmed by experimental data.

Keywords: Prion diseases; Prion proliferation; Solution persistence; Nucleated polymerization mechanism

1. Introduction

Though widely investigated, the pathogenesis of transmissible spongiform encephalopathies (TSEs) remains incompletely understood. These diseases, members of the fatal neurodegenerative disease family, have different names depending on the mammalian species. They are called scrapie for sheep or bovine spongiform encephalopathy (BSE) for cattle, and for humans they appear under forms called kuru, Creutzfeldt–Jakob disease (CJD), Gerstmann–Sträussler–Scheinker syndrome and fatal familial insomnia. It is believed that they show common pathologies such as spongiform degeneration, described as large vacuoles in the cortex and the cerebellum (Horwich and Weissman, 1997). They are also characterized by long incubation periods, a lack of immune response and invisibility to detection as viruses. It has been shown that only one infectious agent is the cause of these diseases (Griffith, 1967; Prusiner, 1982). This agent is the prion; its discovery was very surprising in the sense that it is thought not to be a virus or any other viroid-like agent but is commonly accepted to be a protein (Aguzzi and Polymenidou, 2004; Prusiner, 1991). The fact that a protein alone can transmit an infectious disease has been a great controversy within the scientific community. However, despite some arguments against this protein-only hypothesis, the prion is now widely regarded as the best explanation for TSEs.

Much progress was made in the 1980s in understanding structural aspects of the different forms of prion protein (Oesch et al., 1985; Prusiner, 1991; Prusiner et al., 1981, 1984). To summarize, we can say that the prion infectious agent is a modified form of a normal protein called PrP^C (prion protein cellular) which is a normal proteinase K-sensitive form of prion protein PrP. Single molecules of the protein PrP^C, which we will refer to as monomers, can normally be found in the human system. Many authors have investigated the functional role of prions (Bounhar et al., 2001; Brandner et al., 1996; Brown et al., 2002; Chiesa et al., 2005; Kim et al., 2004; Li and Harris, 2005; Roucou et al., 2003, 2004). Brandner et al. (1996) showed that PrP^{Sc} does not directly damage neurons. Roucou et al. (2003, 2004) showed that for human neurons, normal PrP located in the cytosol retains its

*Corresponding author.
E-mail addresses: mgreer@bates.edu (M.L. Greer), pujo@math.univ-lyon1.fr (L. Pujo-Menjouet), glenn.f.webb@vanderbilt.edu (G.F. Webb).

0022-5193/$ - see front matter © 2006 Elsevier Ltd. All rights reserved.
doi:10.1016/j.jtbi.2006.04.010

protective function against Bax, a substance in the human cell which when activated provokes cell apoptosis. In other words, normal PrP could be considered a natural protection against apoptosis. Without it, a massive destruction of our neurons would occur under stress.

On the other hand, the infectious protein PrP^{Sc} (Prion Protein Scrapie) is an abnormal pathogenic conformation of PrP^{C} and is the origin of the TSEs. PrP^{Sc} is hydrophobic and has a tendency to form aggregates (Prusiner, 1998). It is then more stable than PrP^{C} and much more resistant to proteolytic treatment as well as radiation and high temperatures (Huang et al., 1984; Pan et al., 1993). The motivation to study the dynamics of these protein populations comes from the research of Roucou et al. (2003) and the authors quoted above, which suggests that the PrP^{Sc} proteins do not directly damage the neurons in the TSEs. Indeed, if we assume that PrP^{Sc} is an aggregate that converts PrP^{C} monomers as it replicates, then the neurons would be damaged because the protection of PrP^{C} disappears and no shield against the Bax within the cell persists. Thus, the more an animal or human is stressed the faster the neurons die (Brown et al., 2002). Obviously, this biological assumption is very simplified here, and there exist other hypotheses regarding the cause of death due to the prion disease.

The objective in this work is to understand the dynamics of the PrP^{C} and PrP^{Sc} populations. Our goal is to develop a basic model incorporating the essential elements of prion disease. We would like to understand under what conditions the PrP^{Sc} population survives while the monomer PrP^{C} population declines, and if such conditions are biologically realistic. In other words, we want to study the stability of the protein populations involved in these diseases. In order to study this behavior we need to consider a sufficiently robust model. Several models to explain the replication process of PrP^{Sc} have been proposed (Cohen et al., 1994; Eigen, 1996; Harper and Lansbury, 1997; Jarrett and Lansbury, 1993; Kulkarni et al., 2003; Laurent, 1997; Masel et al., 1999; Mobley et al., 2003; Nowak et al., 1998; Pöschel et al., 2003; Slepoy et al., 2001). These models are distinguished primarily as one-dimensional (lengthening fibrils) or two-dimensional (planar aggregates). Areal aggregation models (that is, two-dimensional aggregations on regular arrays corresponding to cell surfaces) have been investigated (Kulkarni et al., 2003; Mobley et al., 2003; Slepoy et al., 2001) and experimental evidence of areal aggregation has been shown (Govaerts et al., 2004; Wille et al., 2002). There is experimental evidence that PrP proteins with glycophospho-inositol (GPI) anchors deleted can yield increased scrapies upon inoculation without disease symptoms (Chesebro et al., 2005). Areal aggregation models have provided an impressive theoretical explanation of the highly reproducible logarithmic correlation of incubation times and inoculum doses, as well as experimentally observed deviations in this relationship at small doses (Kulkarni et al., 2003).

The view that PrP^{Sc} aggregates are essentially one-dimensional fibrillic structures lengthening in both linear directions has been investigated (Jarrett and Lansbury, 1993; Collins et al., 2004; Lansbury and Caughey, 1981; Scheibel et al., 2001). Collins et al. (2004) investigate one-dimensional yeast prion aggregation by single molecule fluorescence measurements, which indicate that fibrils grow by monomer addition. The one-dimensional propagation of prion fibrils has been modeled mathematically (Masel et al., 1999; Nowak et al., 1998; Pöschel et al., 2003). Masel et al. (1999) hypothesize nucleated polymerization (see Fig. 1) as the primary mechanism of PrP^{Sc} proliferation and develop a deterministic model for it consisting of an infinite system of ordinary differential equations, one for each possible fibril length. The model in Masel et al. (1999) is the starting point of our investigation, but we consider a continuum of possible fibril lengths described by partial differential equations (Greer, 2002). The advantages of our modeling approach are that it is conceptually more accessible and mathematically more tractable.

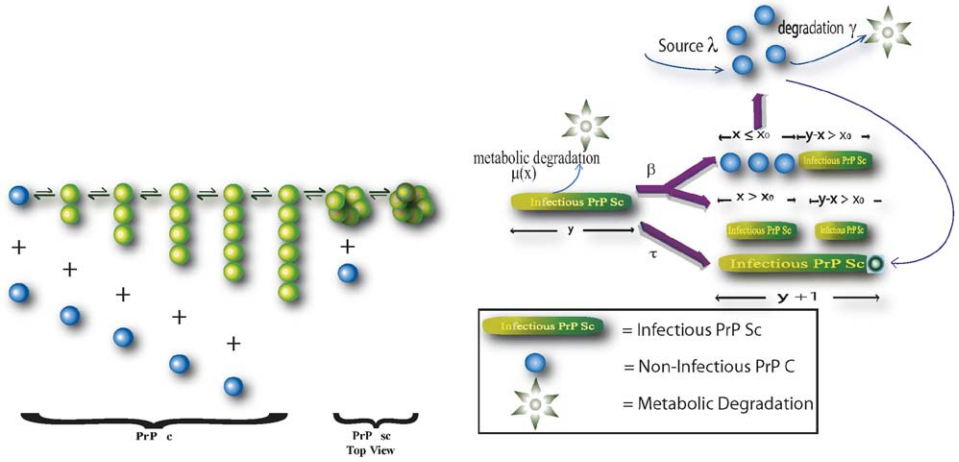

Fig. 1. Left: nucleated polymerization mechanism with minimum nucleation size $n = 6$. Right: Kinetic model of the prion aggregate growth model based on Fig. 2 of Masel et al. (1999).

We state our model of prion proliferation, then find the steady state values of the system. We study the local stability of the disease free and disease steady states. We prove global stability for the disease free steady state and the conditions necessary for persistence of the disease. We conclude with numerical simulations based on experimental data (Masel et al., 1999; Rubenstein et al., 1991). All the details of the proofs of our propositions concerning the existence, uniqueness, and asymptotic behavior of the solutions of the model are available on request.

2. The model of prion proliferation

Our model describes nucleated polymerization, the mechanism by which prions are hypothesized to replicate (Nowak et al., 1998). It is necessarily abstract, because it describes an extremely complex biological process. The model contains six basic parameters, each of which has a fundamental biological interpretation. The nucleated polymerization theory considers the PrP^{Sc} protein to be a polymeric form of PrP^{C}. It is important to point out that above a critical size, PrP^{Sc} is very stable and does not polymerize anymore (Pan et al., 1993). Only terminally truncated forms of the PrP^{Sc} polymerize. Our work is consequently focused on these truncated forms that polymerize which by language abuse we name PrP^{Sc}. By polymerizing, we mean that PrP^{Sc} increases its length by attaching to its end units of converted PrP^{C} in a stringlike formation (Scheibel et al., 2001). After a PrP^{Sc} polymer attaches to a PrP^{C} monomer, the PrP^{C} is converted to the infectious PrP^{Sc} form. It is assumed that the PrP^{Sc} proteins are long enough to wrap into a helical shape, in which they form stabilizing bonds (Wille et al., 2002). The first winding of the helix, achieved at the critical size, is the "nucleus" referred to by the term nucleated polymerization (see Fig. 1) (Masel et al., 1999).

The bonds formed in a PrP^{Sc} polymer likely confer PrP^{Sc} greater metabolic stability than PrP^{C} (Masel et al., 1999). This difference in stability is manifested in the parameters for metabolic degradation of PrP^{Sc} and PrP^{C}. Polymers of PrP^{Sc} can split into smaller polymers, and the mechanisms of lengthening and splitting are the basis of prion proliferation (see Fig. 1). A split usually transforms one infectious polymer into two smaller infectious polymers, each of which can attach PrP^{C}. However, when a newly split polymer falls below the critical size, it immediately degrades into PrP^{C} monomers. We note that our assumption that the PrP^{Sc} polymers can degrade into PrP^{C} units is controversial, although there is experimental evidence that monomers less than a minimum size are energetically unfavorable (Pöschel et al., 2003; Wille et al., 2002). All our results, however, are valid with or without this assumption, that is, our minimum viable polymer length may be as small as 1.

2.1. The monomer population

Let us denote by $V(t)$ the population of PrP^{C} monomers at time $t>0$, and by $U(t)=\int_{x_0}^{\infty} u(x,t)\,dx$ the total population of polymers of length x greater than a minimum length $x_0>0$. The function u is the density of polymers at time $t>0$ with respect to the length $x\in(x_0,\infty)$. Note that polymer lengths have been shown to range over thousands of monomer units (Masel et al., 1999; Prusiner, 1986). In (Masel et al., 1999) polymer lengths x were assumed to be integer values, but we assume continuous values for mathematical tractability. The monomer population satisfies the ordinary differential equation

$$\frac{dV(t)}{dt}=\lambda-\gamma V(t)-\tau V(t)U(t)+2\int_0^{x_0} x\int_{x_0}^{\infty}\beta(y)\kappa(x,y)u(y,t)\,dy\,dx, \tag{1}$$

where $\lambda>0$ is the constant background source of monomers, $\gamma>0$ is the constant metabolic degradation rate of monomers and τ is the polymerization rate, i.e. the rate at which polymers attach to, and convert, monomers. In the last term of the right-hand side, $\beta(y)$ gives the possibly length-dependent likelihood of splitting of polymers to monomers. Supposing a split occurs, $\kappa(x,y)$ is the probability of an polymer of length y splitting to any shorter length x with the other piece having length $y-x$, and is defined in the following way:

$$\kappa(x,y)=\begin{cases}0 & \text{if } y\leqslant x_0 \text{ or } y\leqslant x,\\ 1/y & \text{if } y>x_0 \text{ and } 0<x<y.\end{cases} \tag{2}$$

The form of Eq. (2) means that the probability a length y splits to any shorter length x is equally likely. Observe that for a fixed value of y,

$$\int_0^{\infty}\kappa(x,y)\,dx=\begin{cases}0 & \text{if } y\leqslant x_0,\\ 1 & \text{if } y>x_0.\end{cases} \tag{3}$$

In Eq. (1), the $\tau V(t)U(t)$ term on the right-hand side represents the loss of monomers as PrP^{C} units are attached to the polymer PrP^{Sc}. The term $2\int_0^{x_0} x\int_{x_0}^{\infty}\beta(y)\kappa(x,y)u(y,t)\,dy\,dx$ represents the monomers gained when a PrP^{Sc} polymer splits with at least one polymer shorter than the minimum length x_0. We assume that such a polymer piece degrades immediately into PrP^{C} units. We also give the initial condition

$$V(0)=V_0, \tag{4}$$

where V_0 is positive.

2.2. The polymer population

The polymer population is described by the following transport equation:

$$\frac{\partial}{\partial t}u(x,t)+\tau V(t)\frac{\partial}{\partial x}u(x,t)=-\mu(x)u(x,t)-\beta(x)u(x,t)+2\int_x^{\infty}\beta(y)\kappa(x,y)u(y,t)\,dy. \tag{5}$$

While the term $\tau V(t)U(t)$ of Eq. (1) represents the loss of PrP^C monomers as they are polymerized, the term $\tau V(t)(\partial/\partial x)u(x,t)$ in Eq. (5) shows the gain in length of PrP^{Sc} due to polymerization. The first term on the right-hand side of Eq. (5) gives the metabolic degradation of PrP^{Sc}. In this paper, for simplicity we assume polymers are equally likely to split anywhere along their length where two protein units join, hence $\beta(x)=\beta x$. We also assume $\mu(x)\equiv\mu$. Note the important roles of β and μ. In our model there is a very small probability that PrP^{Sc} polymers can grow to greater lengths than have been experimentally observed. Careful choices of both β and μ can render this probability negligible. These choices do not contradict the biological observations and without them, the study of the model could become extremely complex. The last two terms of Eq. (5) describe splitting. The term $\beta(x)u(x,t)$ is the loss of polymers, subject to the splitting rate $\beta(x)$. The last term of the right-hand side is the count of all the polymers of length x resulting from the splitting of polymers of length greater than x. We give the initial condition for the polymer population as

$$u(x,0)=\varphi(x) \quad \text{for } x_0<x<\infty, \tag{6}$$

and the boundary condition to be

$$u(x_0,t)=0 \quad \text{for } t\geqslant 0. \tag{7}$$

3. An associated system of ordinary differential equations

From the system comprised of Eq. (1) and Eqs. (4)–(7), a straightforward computation allows us to deduce the following associated system of ordinary differential equations:

$$\begin{cases} \dfrac{\mathrm{d}}{\mathrm{d}t}U(t)=\beta P(t)-\mu U(t)-2\beta x_0 U(t),\\ \dfrac{\mathrm{d}}{\mathrm{d}t}V(t)=\lambda-\gamma V(t)-\tau V(t)U(t)+\beta x_0^2 U(t),\\ \dfrac{\mathrm{d}}{\mathrm{d}t}P(t)=\tau V(t)U(t)-\mu P(t)-\beta x_0^2 U(t), \end{cases} \tag{8}$$

where $P(t)=\int_{x_0}^{\infty} xu(x,t)\,\mathrm{d}x$ is the total population of PrP^{Sc} monomers comprising the polymers at time t. We remark that System 8 is analogous to the system of three differential equations presented by Masel et al. (1999). However, in our work, we analyse different aspects of the system. Further, System 8 is obtained from Eq. (1) and Eqs. (4)–(7), which is a formulation of the model based on continuous fibril lengths. The System Eq. (1) and Eqs. (4)–(7) carries more biological information, namely the distribution of prion fibrils, as well as the lengthening and splitting processes.

There are two steady states for System (8): the disease free steady state

$$\overline{U}=0, \quad \overline{V}=\lambda/\gamma \text{ and } \overline{P}=0,$$

and the prion disease steady state

$$\overline{U}=\frac{\beta\lambda\tau-\gamma(x_0\beta+\mu)^2}{\mu\tau(2x_0\beta+\mu)}, \quad \overline{V}=\frac{(x_0\beta+\mu)^2}{\beta\tau}$$

and

$$\overline{P}=\frac{\beta\lambda\tau-\gamma(x_0\beta+\mu)^2}{\beta\mu\tau}.$$

Note that the disease steady state exists only if $x_0\beta+\mu<(\beta\lambda\tau/\gamma)^{1/2}$. The left-hand side of this inequality is related to the net loss of PrP^{Sc} polymers due to their degradation and splitting to unstable lengths, and the right-hand side is related to the net production of polymers due to their lengthening and splitting to stable lengths as they consume the available supply of PrP^C, in other words, the inequality conditioning the disease steady state can be interpreted in terms of the degradation, splitting and lengthening rates of the polymers. We state below results concerning the existence, uniqueness and the partial differential equations Systems Eq. (1) Eqs. (4)–(7). We also state results concerning the stability of the steady state of these two systems. The proofs of Propositions 3.0.1(i) and (ii) are available in the Appendix. The proof of Proposition 3.0.1(iii) is given in Prüss et al. (2006). The proof of Proposition 3.0.2 is based on the results for the associated system of ordinary differential equations and is given in Engler et al. (2006).

Proposition 3.0.1. *Let* $\lambda,\gamma,\tau,\beta,\mu,x_0>0$. *Let* $X=\{(U,V,P)\in\mathbb{R}^3_+ : U\geqslant 0, V\geqslant 0 \text{ and } P\geqslant x_0U\}$

(i) *For each* $(U(0),V(0),P(0))\in X$ *there is a unique solution* $(U(t),V(t),P(t))$ *to the initial value problem* (8) *for* $t\geqslant 0$. *Further*, $(U(t),V(t),P(t))\in X$ *for* $t\geqslant 0$.

(ii) *The disease free steady state given by* $(\overline{U},\overline{V},\overline{P})=(0,\lambda/\gamma,0)$ *is globally stable in* X *for the system* (8) (*that is*, $\lim_{t\to\infty}(U(t),V(t),P(t))=(\overline{U},\overline{V},\overline{P})$ *for all* $(U(0),V(0),P(0))\in X$, *if*

$$(\beta\lambda\tau/\gamma)^{1/2}<x_0\beta+\mu.$$

(iii) *The disease steady state given by*

$$\overline{U}=\frac{\beta\lambda\tau-\gamma(x_0\beta+\mu)^2}{\mu\tau(2x_0\beta+\mu)}, \quad \overline{V}=\frac{(x_0\beta+\mu)^2}{\beta\tau}$$

and

$$\overline{P}=\frac{\beta\lambda\tau-\gamma(x_0\beta+\mu)^2}{\beta\mu\tau}$$

is globally stable in X *for the system* (8), *if*

$$(\beta\lambda\tau/\gamma)^{1/2}>x_0\beta+\mu.$$

Proposition 3.0.2. *Let* $\lambda,\gamma,\tau,\beta,\mu,x_0>0$. *Let* $X=\mathbb{R}\times L_1((x_0,\infty);x\,\mathrm{d}x)$. *For each* $(V_0,\phi)\in X_+$ *there is a unique solution* $(V(t),u(.,t))$ *to the initial value problem System*

Eq. (1) *and Eqs.* (4)–(7) *for* $t \geqslant 0$ *and* $(V(t), U(t), P(t)) \in X_+$. *The disease free steady state* $(\lambda/\gamma, 0)$ *is globally stable in* X_+, *if*

$$(\beta\lambda\tau/\gamma)^{1/2} < x_0\beta + \mu.$$

The disease steady state

$$\overline{V} = \frac{(x_0\beta+\mu)^2}{\beta\tau},$$

$$\overline{u}(x) = \frac{2\beta(\lambda\beta\tau - \gamma(\mu+\beta x_0)^2)}{\mu\tau(\mu+\beta x_0)(\mu+2\beta x_0)}\Phi\left(\frac{\beta(x-x_0)}{\mu+\beta x_0}\right),$$

where $\Phi(r) = (r + r^2/2)\exp(-(r + r^2/2))$, *is globally stable in* X_+, *if*

$$(\beta\lambda\tau/\gamma)^{1/2} > x_0\beta + \mu.$$

4. Numerical illustrations

Our model can be used for simulations based on experimental data for prion proliferation. The model has six parameters: $x_0, \gamma, \lambda, \mu, \beta$, and τ. The minimum stable polymer length x_0 is estimated as 6 to 30 in Masel et al. (1999), but remains controversial (Masel et al., 2005). The half-life of PrP^C monomers is estimated as 3–6 h from studies for mouse neuroblastoma cells (Borchelt et al., 1990; Caughey et al., 1989) which means $\gamma \approx 3-5\,\text{day}^{-1}$. We estimate the PrP^C source as $\lambda \approx 10^3 - 10^4$, which is consistent with the values in Masel et al. (1999). These three parameters x_0, γ, λ are obtainable independently of the disease dynamics. We note that the pre-inoculation steady state $V(0) = \lambda/\gamma$ relates λ and γ independently of the disease dynamics. The other three parameters μ, β, τ can be obtained experimentally from the observed disease steady state values

$$\overline{V} = \frac{(x_0\beta+\mu)^2}{\beta\tau},$$

$$\overline{U} = \frac{\beta\lambda\tau - \gamma(x_0\beta+\mu)^2}{\mu\tau(2x_0\beta+\mu)},$$

$$\overline{P}/\overline{U} = \frac{2x_0\beta+\mu}{\beta},$$

which are, respectively, the monomer population, the polymer population, and the mean polymer length at disease steady state. These three equations yield a unique solution for μ, β, and τ in terms of x_0, λ, γ, $\overline{U}$, $\overline{V}$ and $\overline{P}$ given by

$$\tau = -\frac{(\overline{P}-\overline{U}x_0)^2(\overline{V}\gamma-\lambda)}{\overline{P}\;\overline{U}\;\overline{V}(\overline{P}-2\overline{U}x_0)}, \quad \mu = \frac{-\overline{V}\gamma+\lambda}{\overline{P}}$$

and

$$\beta = \frac{\overline{U}(-\overline{V}\gamma+\lambda)}{\overline{P}(\overline{P}-2\overline{U}x_0)}.$$

We apply our model to experimental data in Rubenstein et al. (1991). The parameter values for the simulation are given in Table 1. MATHEMATICA code used in the simulations is available on request.

4.1. Convergence of the density $u(x,t)$ to the disease steady state

In Fig. 2, the early (left panel) and late (right panel) stages for the pathogenesis of prion proliferation are given for the polymer density $u(x,t)$. It can be seen in Fig. 2 and also in Fig. 3 that the mean polymer length first increases and then decreases as it stabilizes over disease progression. Our model explains this phenomenon as follows. In the early stage there is an abundance of PrP^C monomers which are maintained at a constant source rate. As this population is consumed by the lengthening and splitting polymers, the mean polymer length is constrained. This is consistent with the hypothesis formulated by Roucou et al. (2003), that is, deaths attributable to prion disease result

Table 1
Model parameters and variables definitions and units. The parameter values were taken from Masel et al. (1999)

Parameter/ variable	Definition	Value	Unit
t	Time	–	days
x	Length of a PrP^{Sc} polymer	–	–
x_0	Minimum polymer length	6	–
$u(x,t)$	Density of polymer lengths	–	SAF/sq*
$U(t)$	Total number of PrP^{Sc} polymers	–	SAF/sq
$V(t)$	Total number of PrP^C monomers	–	–
$P(t)$	Total number of PrP^{Sc} monomers in polymers	–	–
γ	Degradation rate of monomers	5	day^{-1}
μ	Degradation rate of polymers	.04	day^{-1}
β	Rate of splitting of polymers to monomers	.0001	$(\text{SAF/sq})^{-1}\text{day}^{-1}$
λ	Source of monomers	4400	day^{-1}
τ	Conversion rate of monomers to polymers	.3	$(\text{SAF/sq})^{-1}\text{day}^{-1}$
$\kappa(x,y)$	Probability that a polymer of length y Splits to lengths x and $y-x$	–	–

*SAF/sq means Scrapie-Associated Fibrils per square unit and is explained in detail by Rubenstein et al. (1991).

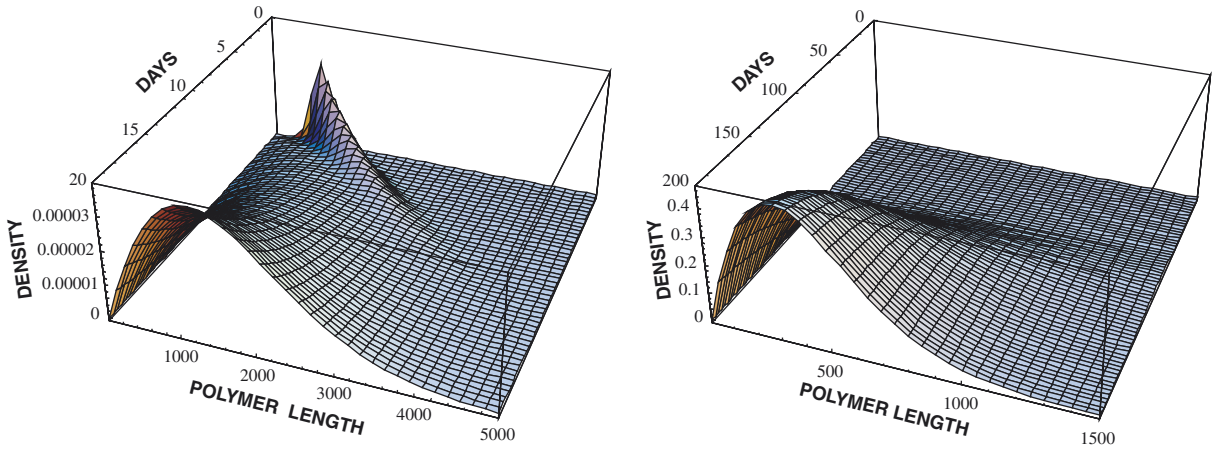

Fig. 2. Evolution of the polymer density distribution $u(x,t)$. For the graph on the left representing the early stage of the proliferation, the mean length of the polymers increases, but then decreases with time. The graph in the right shows the stabilization of the polymer population as $u(x,t)$ converges to the disease steady state. The parameters used are presented in Table 1. The simulations assume an initial PrP^C population $V_0 = 880$ and an initial PrP^{Sc} population $u(y,0)$ given by .000002 times a Gaussian distribution with mean .15 and standard deviation .03.

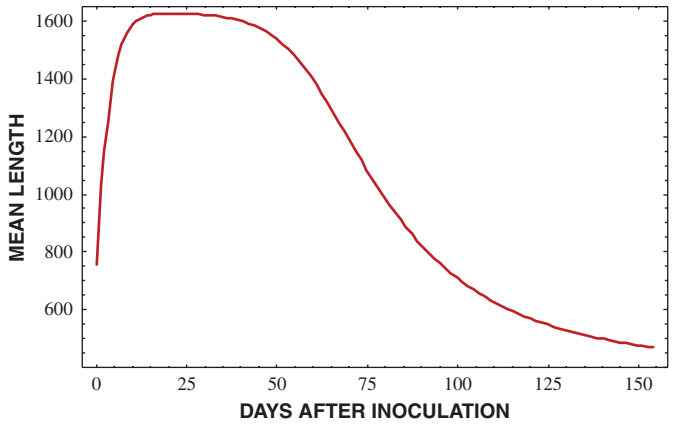

Fig. 3. Evolution of the mean length $P(t)/U(t)$ of the polymer as a function of the days after inoculation. The length of an average polymer increases fast initially and then slowly decreases due to the depletion of the PrP^C monomer population. The parameters used are presented in Table 1. The simulations assume an initial PrP^C population $V_0 = 880$ and an initial PrP^{Sc} population $u(y,0)$ given by .000002 times a Gaussian distribution with mean .15 and standard deviation .03.

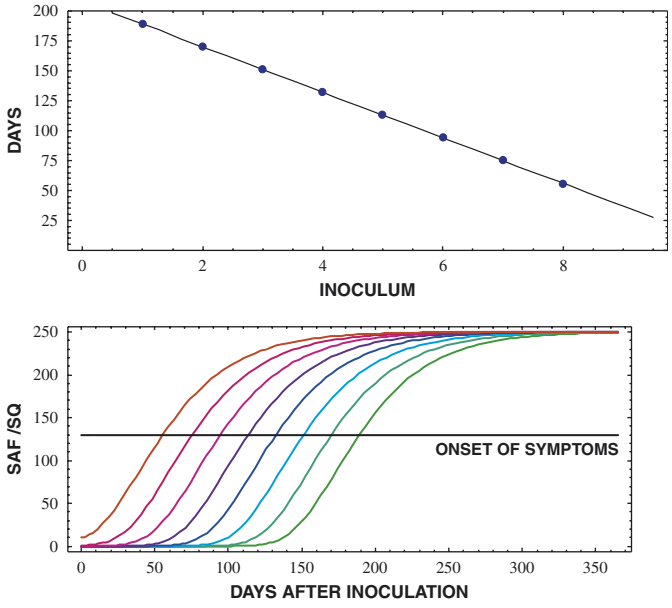

Fig. 4. Top figure: Incubation times in days for inoculum doses $U(0)$ diluted through nine orders of magnitude. All the points are linearly dependent on the log scale. Bottom panel: graphs of the number of fibrils $U(t)$ (in SAF/sq) for the nine inoculum doses. The horizontal line corresponds to the onset of symptoms. The parameters are taken from Table 1.

from the pathogenic consumption of normal PrP^C monomers. Both simulations assume an initial PrP^C population $V_0 = 880$ and an initial PrP^{Sc} population $u(y,0)$ given by .000002 times a Gaussian distribution with mean .15 and standard deviation .03.

4.2. Analysis of infectivity

In Fig. 4 we show the dependence of the incubation time on the inoculation dose. It is well documented (Prusiner, 1986; Ferreira et al., 2003) that the incubation time (defined as appearance of disease symptoms or death) is a log function of the inoculum dose. In the top panel of Fig. 4 the incubation time in days is graphed for nine order of magnitude dilutions of the inoculum dose $U(0)$. In the bottom panel of Fig. 4 the corresponding graphs of $U(t)$ are given. The incubation time is defined as the number of days for $U(t)$ to reach 130 SAF/sq which is the experimental value obtained in Rubenstein et al. (1991) for the appearance of symptoms in mice injected intracerebrally with 139A scrapie strain as measured in spleen.

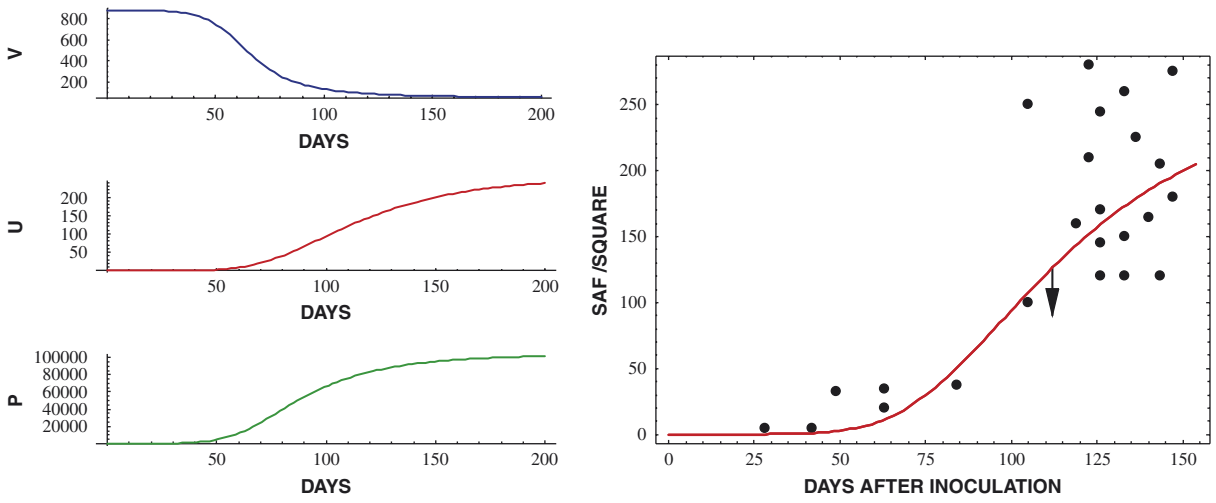

Fig. 5. Left panel: convergence of $V(t)$, $U(t)$ and $P(t)$ to the steady states $\overline{V}$, $\overline{U}$ and $\overline{P}$, with the parameters taken from Table 1. Right panel: scrapie-associated fibrils (SAF) measurements at various times after intracerebral injection of the 139A scrapie strain into Compton white mice (*points*). The solution $U(t)$ of (8) is shown with parameters taken from Table 1, and the experimental data come from Rubenstein et al. (1991). The arrow indicates the time of onset of clinical disease.

In Fig. 5 we graph the solution of System (8) for an inoculum dose corresponding to data in Rubenstein et al. (1991). The model simulation fits the data for the disease progression. This data has also been simulated by Pöschel et al. (2003) who used a model similar to Masel et al. (1999). In Rubenstein et al. (1991) the authors used scrapie-associated fibrils (SAF) as the indicator of infectivity. In their experiment, they infected mice by intracerebral injection as well as intraperitoneal injection then measured the level of SAF in the brain and spleen at various times after inoculation. The data they obtained are shown in Fig. 5 (dots in the graph of the right part, the arrow represents the onset of clinical disease). Here we show the data from the spleen after an intracerebral injection (Fig. 2 in Rubenstein et al. (1991)).

5. Conclusion

We have presented a model of prion proliferation with biological assumptions similar to those of Masel et al. (1999). Our model differs from theirs in that we consider prion polymer length to be a continuous rather than discrete structure variable. This change from a discrete model allows us to show different behaviors of the interacting protein populations. As one example, our model shows the complete polymer distribution $u(x,t)$ for each time t.

The continuous model is simple enough to provide clear numerical results and be easily manipulated, and it is detailed enough to describe many aspects of prion diseases. It is accurate and consistent when compared to biological data. We can use the model to predict events, such as the early increase and later decrease in mean polymer length (Fig. 3), the log relationship between inoculation doses and incubation times (Fig. 4) and the saturation of total PrP^{Sc} mass as a determinant of onset of clinical symptoms (Fig. 5). Yet the model is mathematically challenging enough to leave open questions for both mathematicians and experimental biologists. These include global stability of the disease steady state and a more complete description of PrP lengths and quantities in vivo.

We have several directions for future work. The model requires analysis in the case when μ and β are not constant and investigation of unstable behavior and possible oscillations. We will study each parameter in more depth to better understand its influence on disease progression. And finally, the model may be adapted to reflect further biological understanding of polymer formation.

Appendix A. Proof of Proposition 3.0.1(i)

We first give the following equivalent system of equations to system (8) in terms of $U(t)$, $V(t)$, $W(t)$, where $W(t) = P(t) - x_0 U(t)$:

$$\begin{cases} \dfrac{\mathrm{d}}{\mathrm{d}t}U(t) = \beta W(t) - (\mu + \beta x_0)U(t), \\ \dfrac{\mathrm{d}}{\mathrm{d}t}V(t) = \lambda - \gamma V(t) - \tau V(t)U(t) + \beta x_0^2 U(t), \\ \dfrac{\mathrm{d}}{\mathrm{d}t}W(t) = \tau V(t)U(t) - (\mu + \beta x_0)W(t). \end{cases}$$

We re-write the new system in vector form as

$$\frac{\mathrm{d}}{\mathrm{d}t}\mathbf{Z}(t) = A\mathbf{Z}(t) + F(\mathbf{Z}(t)), \quad \mathbf{Z}(0) = (U(0), V(0), W(0)), \tag{9}$$

where $\mathbf{Z}(t) = (U(t), V(t), W(t))^{\mathrm{T}}$, A is the matrix defined by

$$A = \begin{pmatrix} -(\mu+\beta x_0) & 0 & \beta \\ \beta x_0^2 & -\gamma & 0 \\ 0 & 0 & -(\mu+\beta x_0) \end{pmatrix}$$

and $F(\mathbf{Z}(t)) = (0, \lambda - \tau U(t)V(t), \tau U(t)V(t))^{\mathrm{T}}$. The integration of Eq. (9) gives

$$\mathbf{Z}(t) = \mathrm{e}^{tA}\mathbf{Z}(0) + \int_0^t \mathrm{e}^{(t-s)A} F(\mathbf{Z}(s))\,\mathrm{d}s, \tag{10}$$

where

$$\mathrm{e}^{tA} = \begin{pmatrix} \mathrm{e}^{-t(\mu+\beta x_0)} & 0 & \mathrm{e}^{-t(\mu+\beta x_0)} t\beta \\ \dfrac{\mathrm{e}^{-t\gamma}(1-\mathrm{e}^{-t(\mu+\beta x_0-\gamma)})\beta x_0^2}{\mu+\beta x_0-\gamma} & \mathrm{e}^{-t\gamma} & \dfrac{\mathrm{e}^{-t(\mu+\beta x_0)} x_0^2\beta^2(\mathrm{e}^{t(\mu+\beta x_0-\gamma)} - 1 - t(\mu+\beta x_0-\gamma))}{(\mu+\beta x_0-\gamma)^2} \\ 0 & 0 & \mathrm{e}^{-t(\mu+\beta x_0)} \end{pmatrix}$$

if $\mu + \beta x_0 \neq \gamma$, and

$$\mathrm{e}^{tA} = \begin{pmatrix} \mathrm{e}^{-t\gamma} & 0 & \mathrm{e}^{-t\gamma} t\beta \\ \mathrm{e}^{-t\gamma} t\beta x_0^2 & \mathrm{e}^{-t\gamma} & \frac{1}{2}\mathrm{e}^{-t\gamma} t^2 x_0^2 \beta^2 \\ 0 & 0 & \mathrm{e}^{-t\gamma} \end{pmatrix}$$

if $\mu + \beta x_0 = \gamma$. Then, $\mathrm{e}^{tA}(\mathbb{R}^3_+) \subset \mathbb{R}^3_+$ for $t \geqslant 0$, F is Lipschitz continuous on bounded sets in $\mathbb{R}^3_+$, and for each $\mathbf{Z} \in \mathbb{R}^3_+$, $\mathbf{Z} + hF(\mathbf{Z}) \in \mathbb{R}^3_+$ for $h > 0$ and sufficiently small. Thus, there exists a unique solution of (9) in $\mathbb{R}^3_+$ for each $\mathbf{Z}(0) \in \mathbb{R}^3_+$ defined on a maximal interval of existence $[0, t_{\max})$, and either $t_{\max} = \infty$ or $t_{\max} < \infty$ and $\lim t \to t^+_{\max} \|\mathbf{Z}(t)\| = \infty$ (Martin, 1976). Since

$$\begin{aligned} &\frac{\mathrm{d}}{\mathrm{d}t}(U(t) + V(t) + W(t)) \\ &\quad = \beta W(t) - (\mu + \beta x_0)(U(t) + W(t)) + \lambda - \gamma V(t) + \beta x_0^2 U(t) \\ &\quad \leqslant \lambda + c(U(t) + V(t) + W(t)) \end{aligned}$$

for some positive constant c, the solution $\mathbf{Z}(t)$ stays bounded on bounded intervals of t. Thus, $t_{\max} = \infty$, and the existence of a unique global positive solution is proved.

Appendix B. Proof of Proposition 3.0.1(ii)

Let us define the mapping $F : C(\mathbb{R}^3_+) \longrightarrow \mathbb{R}$ by

$$F(U, V, P) = \left(V - \frac{\lambda}{\gamma}\right)^2 + bU + \frac{\beta b}{\mu} P,$$

with

$$b = \frac{1}{\beta^2\gamma\tau}(2\mu(4x_0\beta\gamma\mu + 2\gamma\mu^2 + \beta(x_0^2\beta\gamma - \lambda\tau))).$$

Then F is a Liapunov functional. Indeed, notice first that the condition $(\beta\lambda\tau/\gamma)^{1/2} < x_0\beta + \mu$ implies that $b > 0$, and thus $(0, \lambda/\gamma, 0)$ is a strict minimum for F. It is not difficult to show that

$$\begin{aligned} \dot{F}(U, V, P) = &-2bUx_0\beta - \frac{\beta b}{\mu} Ux_0^2\beta + 2UVx_0^2\beta \\ &- 2V^2\gamma + 4V\lambda - 2\frac{Ux_0^2\beta\lambda}{\gamma} - 2\frac{\lambda^2}{\gamma} - bU\mu \\ &+ \frac{\beta b}{\mu} UV\tau - 2UV^2\tau + 2\frac{UV\lambda\tau}{\gamma} \end{aligned}$$

and then,

$$\begin{aligned} \dot{F}(U, V, P) \leqslant -\frac{U}{\gamma}\Bigg(&b\gamma(2x_0\beta + \mu) + \left(\frac{\beta b\gamma}{\mu}\gamma + 2(-V\gamma + \lambda)\right) \\ &\times (x_0^2\beta - V\tau)\Bigg), \end{aligned}$$

which for b given above and from the condition $(\beta\lambda\tau/\gamma)^{1/2} < x_0\beta + \mu$, leads to

$$\dot{F}(U, V, P) \leqslant 0.$$

Then from Hale (1969) the proof is complete.

References

Aguzzi, A., Polymenidou, M., 2004. Mammalian prion biology: one century of evolving concepts. Cell 116, 313–327.

Borchelt, D.R., Scott, M., Taraboulos, A., Stahl, N., Prusiner, S.B., 1990. Scrapie and cellular prion proteins differ in their kinetics of synthesis and topology in cultured cells. J. Cell Biol. 110, 743–752.

Bounhar, Y., Zhang, Y., Goodyer, C., LeBlanc, A., 2001. Prion protein protects human neurons against bax-mediated apoptosis. J. Biol. Chem. 276, 39145–39149.

Brandner, S., Isenmann, S., Raeber, A., Fischer, M., Sailer, A., Kobayashi, Y., Marino, S., Weissmann, C., Aguzzi, A., 1996. Normal host prion protein necessary for scrapie-induced neurotoxicity. Nature 379, 339–343.

Brown, D., Nicholas, R., Canevari, L., 2002. Lack of prion protein expression results in a neuronal phenotype sensitive to stress. J. Neurosci. Res. 67, 211–224.

Caughey, B., Race, R.E., Ernst, D., Buchmeier, M.J., Chesebro, B., 1989. Prion protein biosynthesis in scrapie-infected and uninfected neuroblastoma cells. J. Virol. 63, 175–181.

Chesebro, B., Trifilo, M., Race, R., Meade-White, K., Teng, C., LaCasse, R., Raymond, L., Favara, C., Baron, G., Priola, S., Caughey, B., Masliah, E., Oldstone, M., 2005. Anchorless prion protein results in infectious amyloid disease without clinical scrapie. Science 308, 1435–1439.

Chiesa, R., Piccardo, P., Dossena, S., Nowoslawski, L., Roth, K.A., Ghetti, B., Harris, D.A., 2005. Bax deletion prevents neuronal loss but not neurological symptoms in a transgenic model of inherited prion disease. Proc. Natl Acad. Sci. USA 102, 238–243.

Cohen, F.E., Huang, Z., Fletterick, R.J., Baldwin, M., Prusiner, S.B., 1994. Structural clues to prion replication. Science 264, 530–531.

Collins, S., Douglass, A., Vale, R., Weissman, J., 2004. Mechanism of prion propagation: amyloid growth occurs by monomer addition. PLOSBio 2, 1582–1590.

Eigen, M., 1996. Prionics or the kinetic basis of prion diseases. Biophys. Chem. 63, 11–18.

Engler, H., Prüss, J., Webb, G.F., 2006. Analysis of a model for the dynamics of prions II, in press.

Ferreira, A.S., da Silva, M.A., Cressoni, J.C., 2003. Stochastic modeling approach to the incubation time of prionic diseases. Phys. Rev. Lett. 90, 198101–198104.

Govaerts, C., Wille, H., Prusiner, S.B., Cohen, F.E., 2004. Evidence for assembly of prions with left-handed β-helices into trimers. Proc. Natl Acad. Sci. 101, 8342–8347.

Greer, M.L., 2002. A population model of prion dynamics. Ph.D. Thesis, Vanderbilt University.

Griffith, J.S., 1967. Nature of the scrapie agent. Nature 215, 1043–1044.

Hale, J., 1969. Ordinary Differential Equations. Wiley-Interscience, New-York.

Harper, J.D., Lansbury, P.T., 1997. Models of amyloid seeding in Alzheimer's disease and scrapie: mechanistic truths and physiological consequences of the time-dependent solubility of amyloid proteins. Ann. Rev. Biochem. 66, 385–407.

Horwich, A.L., Weissman, J.S., 1997. Deadly conformations: protein misfolding in prion disease. Cell 89, 499–510.

Huang, Z.W., Gabriel, J.M., Baldwin, M.A., Fletterick, R.J., Prusiner, S.B., ECohen, F., 1984. Proposed three-dimensional structure for the cellular prion protein. Proc. Natl Acad. Sci. USA 47, 71–79.

Jarrett, J.T., Lansbury, P.T., 1993. Seeding "one-dimensional crystallization" of smyloid: a pathogenic mechanism in Alzheimer's disease and scrapie? Cell 73, 1055–1058.

Kim, B.H., Lee, H.G., Choi, J.K., Kim, J.I., Choi, E.K., Carp, R.I., Kim, Y.S., 2004. The cellular prion protein (prpc) prevents apoptotic neuronal cell death and mitochondrial dysfunction induced by serum deprivation. Mol. Brain Res. 124, 40–50.

Kulkarni, R.V., Slepoy, A., Singh, R.R.P., Cox, D.L., Pázmándi, F., 2003. Theoretical modeling of prion disease incubation. Biophys. J. 85, 707–718.

Lansbury, P., Caughey, B., 1981. The chemistry of scrapie infection: implication of the "ice 9" metaphor. Chem. Biol. 2, 1–5.

Laurent, M., 1997. Autocatalytic processes in cooperative mechanisms of prion diseases. FEBS Lett. 407, 1–6.

Li, A., Harris, D.A., 2005. Mammalian prion protein suppresses bax-induced cell death in yeast. J. Biol. Chem. 280, 17430–17434.

Martin, R.H., 1976. Nonlinear Operators and Differential Equations in Banach Spaces. Wiley Interscience Series of Texts, Monographs & Tracts, New York.

Masel, J., Jansen, V.A.A., Nowak, M.S., 1999. Quantifying the kinetic parameters of prion replication. Biophys. Chem. 77, 139–152.

Masel, J., Genoud, N., Aguzzi, A., 2005. Efficient inhibition of prion replication by prp-fc$_2$ suggests that the prion is a prp^{Sc} oligomer. J. Mol. Biol. 345, 1243–1251.

Mobley, D.L., Cox, D.L., Singh, R.R., Kulkarni, R.V., Slepoy, A., 2003. Simulations of oligomeric intermediates in prion diseases. Biophys. J. 85, 2213–2223.

Nowak, M.A., Krakauer, D.C., Klug, A., May, R.M., 1998. Prion infection dynamics. Integr. Biol. 1, 3–15.

Oesch, B., Westaway, D., Walchli, M., McKinley, M.P., Kent, S.B.H., Aebersold, R., Barry, R.A., Tempst, P., Teplow, D.B., Hood, L.E., Prusiner, S.B., Weissmann, C., 1985. A cellular gene encodes scrapie prp 27–30 protein. Cell 40, 735–746.

Pan, K.M., Baldwin, M., Nguyen, J., Gasset, M., Serban, A., Groth, D., IlMelhorn, S., Huang, Z., Fletterick, R.J., Cohen, F.E., Prusiner, S.B., 1993. Conversion of α-helices into β-sheets features in the formation of the scrapie prion proteins. Proc. Natl Acad. Sci. USA 90, 10962–10966.

Pöschel, N., Brilliantov, V., Frommel, C., 2003. Kinetics of prion growth. Biophys. J. 85, 3460–3474.

Prusiner, S.B., 1982. Novel proteinaceous infectious particles cause scrapie. Science 216, 136–144.

Prusiner, S.B., 1986. Prions. Sci. Am. 4, 50–59.

Prusiner, S.B., 1991. Molecular biology of prion diseases. Science 252, 1515–1522.

Prusiner, S.B., 1998. Prions. Proc. Natl Acad. Sci. USA 95, 13363–13383.

Prusiner, S.B., McKinley, M.P., Groth, D.F., Bowman, K.A., Mock, N.I., Cochran, S.P., Masiarz, F.R., 1981. Scrapie agent contains a hydrophobic protein. Proc. Natl Acad. Sci. USA 78, 6675–6679.

Prusiner, S.B., Groth, D.F., Bolton, D.C., Kent, S.B., Hood, L.E., 1984. Purification and structural studies of a major scrapie prion protein. Cell 38, 127–134.

Prüss, J., Pujo-Menjouet, L., Webb, G.F., Zacher, R., 2006. Analysis of a model for the dynamics of prions. Discrete Control Dyn. Syst. Ser. B 6 (1), 215–225.

Roucou, X., Guo, Q., Zhang, Y., Goodyer, C.G., Leblanc, A., 2003. Cytosolic prion protein is not toxic and protects against bax-mediated cell death in human primary neurons. J. Biol. Chem. 278, 40877–40881.

Roucou, X., Gains, M., Leblanc, A.C., 2004. Neuroprotective functions of prion protein. J. Neuroscience Res. 75, 153–161.

Rubenstein, R., Merz, P.A., Kascsak, R.J., Scalici, C.L., Papini, M.C., Carp, R.I., Kimberlin, R.H., 1991. Scrapie-infected spleens: analysis of infectivity, scrapie-associated fibrils, and protease-resistant proteins. J. Infect. Dis. 164, 29–35.

Scheibel, T., Kowal, A.S., Bloom, J.D., Lindquist, S.L., 2001. Bidirectional amyloid fiber growth for a yeast prion determinant. Curr. Biol. 11, 366–369.

Slepoy, A., Kulkarni, R.V., Singh, R.R.P., Pázmándi, F., Cox, D.L., 2001. On the statistical mechanics of prion proteins. Phys. Rev. Lett. 87, 8101–8104.

Wille, H., Michelitsch, M.D., Guenebaut, V., Supattapone, S., Serban, A., Cohen, F.E., Agard, D.A., Prusiner, S.B., 2002. Structural studies of the scrapie prion protein by electron crystallography. Proc. Natl Acad. Sci. USA 99, 3563–3568.

Further reading

Simonett, G., Walker, C. On the solvability of a mathematical model for prion proliferation. J. Math. Anal. Appl., to appear.